Journal Pre-proofs

Full Length Article

Study of damage mechanism on single crystal 4H-SiC surface layer by picosecond laser modification (PLM)

Haixu Liu, Zhipeng Li, Ping Zhang, Dunwen Zuo, Wenkun Xie

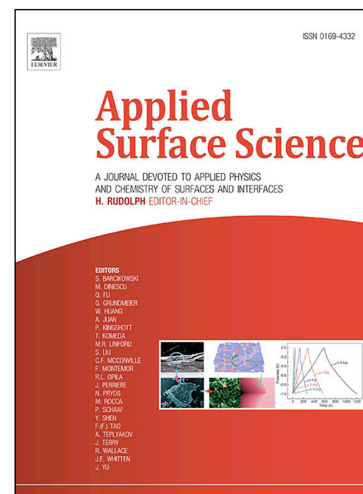

PII: S0169-4332(24)01435-1
DOI: https://doi.org/10.1016/j.apsusc.2024.160722
Reference: APSUSC 160722

To appear in: *Applied Surface Science*

Received Date: 23 April 2024
Revised Date: 30 June 2024
Accepted Date: 9 July 2024

Please cite this article as: H. Liu, Z. Li, P. Zhang, D. Zuo, W. Xie, Study of damage mechanism on single crystal 4H-SiC surface layer by picosecond laser modification (PLM), *Applied Surface Science* (2024), doi: https://doi.org/10.1016/j.apsusc.2024.160722

This is a PDF file of an article that has undergone enhancements after acceptance, such as the addition of a cover page and metadata, and formatting for readability, but it is not yet the definitive version of record. This version will undergo additional copyediting, typesetting and review before it is published in its final form, but we are providing this version to give early visibility of the article. Please note that, during the production process, errors may be discovered which could affect the content, and all legal disclaimers that apply to the journal pertain.

© 2024 Published by Elsevier B.V.

Study of damage mechanism on single crystal 4H-SiC surface layer by picosecond laser modification (PLM)

Haixu Liu[a], Zhipeng Li[a,*], Ping Zhang[a], Dunwen Zuo[a,*], Wenkun Xie[b]
[a] College of Mechanical and Electrical Engineering, Nanjing University of Aeronautics and Astronautics, Nanjing, 210000, Jiangsu, China.
[b] University of Strathclyde. Glasgow, Scotland, The United Kingdom of Great Britain and Northern Ireland.

Abstract: The stable structure, high hardness, and brittleness of single-crystal 4H-SiC present challenges in achieving efficient and damage-free polishing processing. Ultra-short pulsed laser-induced surface modification provides a new solution to enhance the manufacturability of 4H-SiC. This paper aims to investigate the underlying mechanism of the picosecond laser-induced surface structural changes in 4H-SiC and the process of material removal from solid to vapour, elucidating the interaction mechanism between picosecond laser and 4H-SiC. A temperature gradient distribution model for picosecond laser irradiation on 4H-SiC was built to reveal the formation mechanism of subsurface crack damage. The results show that a combination of phase explosion and thermal effects controlled picosecond laser-modified 4H-SiC surfaces deposited spherical SiO_2 particles and the process. The study demonstrates that the cracking behaviour in the subsurface of picosecond laser-modified SiC predominantly occurs in the recast region. The fundamental cause of cracking is attributed to the tensile stresses generated by thermal effects and the volumetric changes in the molten material resulting from the overlapping of neighbouring spots in alternating hot-cold cycles. The nanoindentation demonstrated that laser modification can effectively enhance the machinability of SiC. The findings of this study can provide a theoretical basis for efficient non-destructive machining of hard and brittle materials.

Keywords: Single-crystal SiC; Picosecond laser; Surface layer modification; subsurface damage

1. Introduction

Silicon carbide has found wide applications in high-power and high-frequency electronics [1-3], thanks to its robust resistance to radiation and adaptability to challenging environments, such as high pressure and high frequency [1]. Nevertheless, it is challenging to achieve high removal rates and excellent surface quality on silicon carbide through conventional processing methods, due to the mechanical hardness and chemical inertness [4-8]. Chemical Mechanical Polishing (CMP) is regarded as one of the most efficient techniques for ultra-precision surface treatment, but its material removal rate is as low as 1 μm/h [9]. It is critical to research novel methods or processes to enhance the manufacturability of Silicon carbide, thereby maximizing the material removal rate and improving surface/subsurface quality.

Certain researchers have suggested surface modification techniques to address the challenges of low polishing efficiency and surface quality on silicon carbide, such as thermal oxidation, plasma electrochemical oxidation, etc [10-12]. Ultra-short pulse lasers are regarded as versatile tools capable of achieving high-precision and efficient processing or modification of diverse materials. As the thermal impact zone of ultra-short pulse lasers is extremely limited, the local stresses can be effectively reduced, thereby contributing to improving surface quality and minimizing cracks and other

* Corresponding author.
E-mail address: zhipeng.li@nuaa.edu.cn (Z. Li), E-mail address: imit505@nuaa.edu.cn (D. Zuo).

Journal Pre-proofs

forms of subsurface damage [13, 14]. Huang [15] et al. achieved improved material machinability through surface decomposition and laser-induced periodic surface structures obtained by modifying SiC surfaces with femtosecond lasers. Additionally, the lowest root-mean-square deviation roughness (Rq) and surface roughness (Ra) were observed within the experimental conditions. Qin [16] et al. used ultrashort pulses to modify magnesium aluminate spinel for assisted polishing, and the results showed a 61% reduction in Ra for the modified relative to the unmodified. Additionally, it is believed that the thermal loading effect of the laser will induce residual thermal stresses in the shallow surface layer of the modified SiC, potentially causing damage to the subsurface and consequently impacting its serviceability. Amsellem [17] et al. employed a femtosecond laser to modify SiC and confirmed through GIXRD detection and Raman-assisted verification that SiC undergoes decomposition while Si undergoes continuous oxidation in a very thin (3 μm) subsurface region. Zahrani [18] et al. employed short-pulse laser-assisted grinding of Si3N4 to examine the occurrence of subsurface porosity and cracks post-laser modification, attributed to thermal stresses, stress-release mechanisms from high-temperature cooling, mismatches in coefficients of thermal expansion between grains and phases along grain boundaries, or localized crystallization of phases along grain boundaries. Hence, it is evident that the laser type results in diverse material removal mechanisms. Molian [19] et al. utilized a picosecond laser to fabricate 10 μm diameter holes on the SiC surface. Analytical results revealed the absence of defects such as cracks and thermal impacts on the edges and sidewalls of the holes, implying Coulomb explosion as the primary material removal mechanism. This underscores the superior ablation rate of picosecond lasers over femtosecond lasers.

Some researchers have investigated the modification mechanism, temperature evolution, and subsurface damage of SiC single-crystal surfaces by employing ultra-short pulse lasers, aiming to achieve controlled surface damage. Chen [20] et al. employed the finite element method (FEM) to investigate the impact of femtosecond laser modification on the surface mechanical properties, removal mechanism, removal efficiency, and microstructural changes during the removal process of 4H-SiC, comparing it with the original 4H-SiC surface. The results suggest that the instability of laser-induced periodic surface structures (LIPSS) and the combined removal modes of the modified layer (plastic deformation and brittle fracture) contribute to stress and scratching force reduction. An [21] et al. investigated the mechanism of SiC periodic structure generation in extreme ultraviolet (EUV) pulse based on molecular dynamics (MD). The results show that the stripe-like structure is formed due to the uneven energy distribution of a beam. The laser-induced periodic surface structure at the close-to-atomic scale is first presented. Long [13] et al. conducted a thorough investigation into the surface integrity and removal mechanism of cutting SiC using a flat-top laser beam. The findings suggest that laser parameters and beam shape are key factors influencing surface integrity. Xie [22] et al. employed ultrafast lasers for the surface modification of SiC in different media. The findings suggest that the incubation effect primarily governs the periodic structure, and the depth of surface modification and polishing removal thickness indicates that the initial damage depth exceeds 8 μm. Additionally, fluctuations in Ra indicate the dominant presence of indentations and subsurface cracks.

Journal Pre-proofs

Meng [23] et al. employed femtosecond laser modification to enhance the machinability of SiC surface layers. Scratch tests confirmed that the debris generated by periodic structure removal is primarily in the form of plastic build-up and block separation, the cracks generated by this form of fragmentation do not extend to the subsurface, thereby improving the removal efficiency of the material and achieving controllable subsurface damage.

In this study, picosecond laser-induced surface modification of 4H-SiC was employed to investigate the effect of laser energy density on surface morphology and sub-surface damage by combining experiments and numerical simulation. The mechanical properties of SiC after laser modification were analysed using nanoindentation. Utilizing the finite element method (FEM), an analysis was conducted to determine the temperature gradient law and the influence mechanism of the temperature field on the formation of sub-surface crack damage.

2. Experimental setup

This study utilized a TruMicro 5050 picosecond laser (Fig. 1a) to modify single-crystal 4H-SiC (Hefei Kejing Material Technology Co., Ltd., China). The focal point was fixed on the 4H-SiC surface, while the entire plane was scanned reciprocally through laser direct writing technology. Following laser modification, angle polishing was undergone on 4H-SiC using the Shenyang ZYP300 gravity polisher (see Fig. 1b) and the utilised polishing parameters are detailed in section 2.2. Fig. 2 illustrates the initial morphology of the laser-modified 4H-SiC surface with a measuring region of 5 × 5 × 0.3 mm^3. This size was chosen to prevent fragmentation of 4H-SiC ingots during cutting due to thinness. It ensures the yield rate of large-size (6-inch) wafers when divided into the required sizes (the sizes used in the text) and prevents issues during subsequent angular polishing. Small sizes may be difficult to polish and may fragment under load. Therefore, this size ensures the smooth progress of the study. Detailed parameters of the picosecond laser and 4H-SiC were provided in Tables 1 and 2, respectively (Please refer to the supplementary file 1 for comments on heat capacity and thermal conductivity).

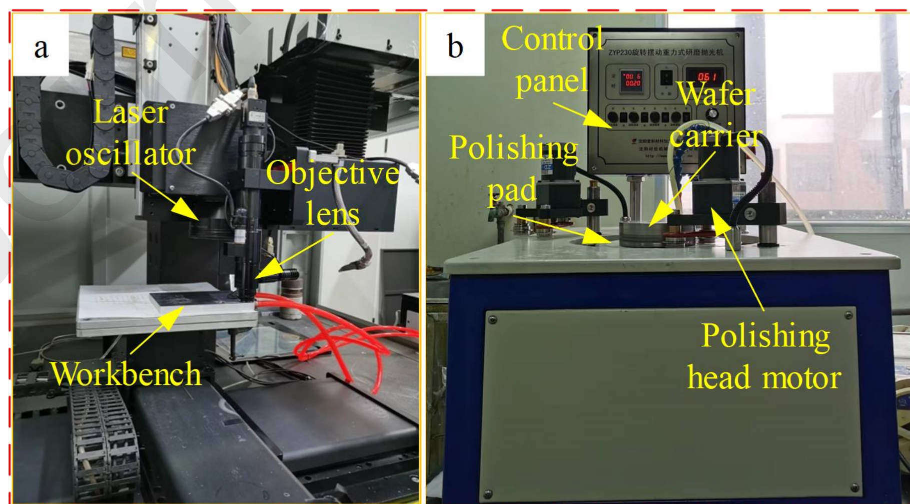

Fig. 1. Laser and angle polishing equipment diagrams: (a) laser equipment diagram; (b) angle polishing equipment diagram.

Journal Pre-proofs

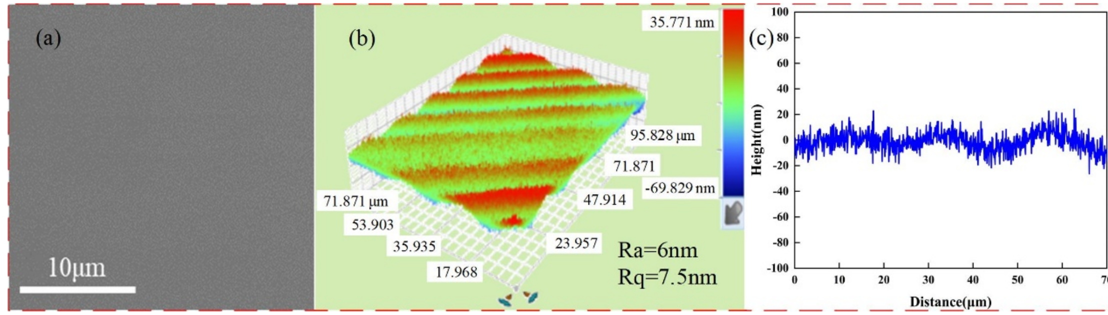

Fig. 2 Initial surface morphology of 4H-SiC: (a) SEM morphology; (b) three-dimensional morphology; (c) the contour corresponding to the three-dimensional morphology.

Table 1 The main specifications of the picosecond laser

Parameters	Values	Experimental parameters
Wavelength	1030nm	1030nm
Laser power	~50W	5, 10, 15, 20 W
Pulse duration	≤10ps	10 ps
spot diameter	20 μm	20 μm
Pulse frequency	100-1000kHz	100 kHz
Beam quality	＜1.3	＜1.3

Table 2 Detail properties of the 4H-SiC

Parameters	Values
Hardness (GPa)	36.8
Elastic modulus (GPa)	543.4
Poisson's ratio	0.2
Density (g/cm^3)	3.2
Heat capacity C_ρ [24, 25] (J/Kg·K)	$\begin{cases} 3517-7357T^{-0.1553} & ;T\le 1200K \\ 1071 & ;T>1200K \end{cases}$
Thermal conductivity k [25, 26] (W/m/K)	$\begin{cases} 451700T^{-0.129} & ;T\le 3100K \\ \dfrac{29900}{T-99} & ;T>3100K \end{cases}$

The aim of this paper is to investigate the effect of energy density on surface layer (surface and subsurface) morphology and damage induced by picosecond laser (pulse width of 10 ps) modification. An overlap of 70% (adjacent track direction) and 90% (scanning direction) helps angle polishing to achieve high removal efficiency and visibility of subsurface morphology in a short time period. Therefore, the angle polishing method is chosen to characterize the subsurface morphology in this paper, as shown in Fig. 3. The angle polishing process uses 12°, and the depth of the damage layer can be calculated from the tangent of the projected length after angle polishing.

Journal Pre-proofs

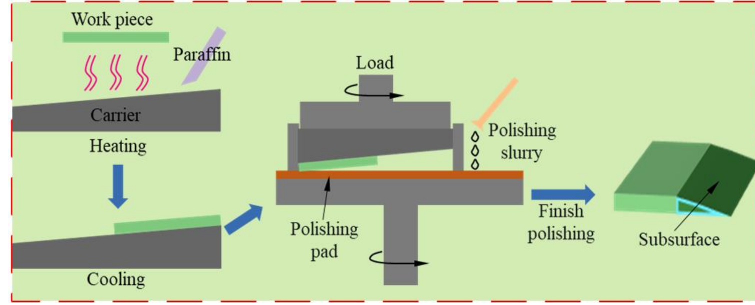

Fig. 3 Schematic illustration of the angle polishing method

Specifically, the laser-modified SiC is affixed to the slide using paraffin. After cooling, a holder is used to fix the position of the slide. By applying a load to the slide, the cross-section is polished using Al_2O_3 slurry. The pressure, polishing disc and workpiece rotation speed, and time for the angle polishing experiments were 13.79 kPa, 60 r/min, and 1.5 h, respectively.

A Bruker surface profiler (Contour GT-K, with a vertical resolution of 0.1 nm) was employed to capture the three-dimensional morphology and profile curves of the SiC surface. Scanning electronic microscopy (SEM) was utilized for observing the surface morphology, and energy dispersive spectroscopy (EDS) was applied to detect the surface element content. The SiC subsurface with different power modifications was etched by X-ray photoelectron spectroscopy (XPS. USA, model: Thermo scientific ESCALAB Xi+) with an argon ion beam to obtain information about their subsurface composition.

3 Temperature field modelling

The transient temperature field generated during the laser modification process has a determinant effect on the surface microstructure and damage mechanism of SiC. In Fig. 5a, it can be seen that during the laser modification of 4H-SiC, the plasma cloud zone, the modified layer, the heat affected zone (HAZ, also known as the liquid phase zone) and the matrix (solid phase zone) can be clearly distinguished. Therefore, this paper develops an axisymmetric two-temperature model using finite element Comsol Multiphysics to solve the temperature fields of electrons and lattices in the time and space domains. In this model, the single-pulse effect of the chemical reaction of the modification process was ignored and the material is also considered isotropic and homogeneous.

As shown in Fig. 5b, the laser beam is simplified to a Gaussian heat source in space and time, and its energy distribution with time in the direction of the machining depth is described by Eq. 1.

$$S(r,z,t)=\frac{4\alpha P}{\pi\omega_0^2 f\tau}exp\left(-4\frac{(x-vt)^2+y^2}{\omega_0^2}-\alpha h+t_{shape}\right) \tag{1}$$

where P is the laser power, α is the SiC absorption coefficient, ω_0 is the beam diameter, f is the pulse frequency, and τ is the pulse width. If we consider the increase of the laser spot radius after the laser is incident on the SiC surface, the heat source shows a conical shape at this time. Neglecting the change in the scattering angle of SiC in beam propagation, the spot radius at the depth of incidence h is described by Eq. 2.

$$\omega_h = \omega_0 \pm h\tan\frac{\theta}{2} \tag{2}$$

The description of ω_h is shown in Fig. 4.

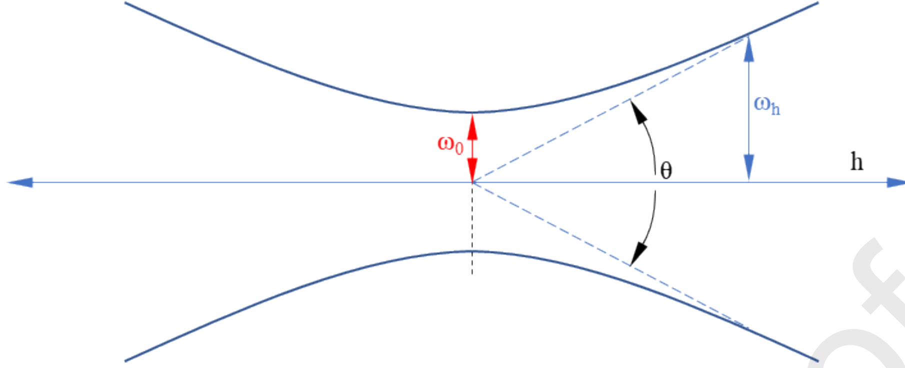

Fig. 4 Variation law of spot diameter with modification depth h

$$S(r,z,t) = \frac{4\alpha P}{\pi\left(\omega_0 + h\tan\frac{\theta}{2}\right)^2 f\tau} exp\left(-4\frac{(x-vt)^2 + y^2}{\left(\omega_0 + h\tan\frac{\theta}{2}\right)^2} - \alpha h + t_{shape}\right) \tag{3}$$

where θ is the Gaussian beam far-field emission angle ($\theta \approx 1.128\ (\lambda/\pi\omega_0)$). The plus and minus signs in the equation take a positive sign when the SiC is located below the focusing plane of the laser beam and a negative sign when it is located above the focusing plane. Therefore, the heat source used in this paper is described in Eq. 3.

Considering the Gaussian distribution of the laser pulse in the time domain (t_{shape}), the time pulse shape function (Eq. 4) can be derived [27].

$$t_{shape} = \begin{cases} exp\left(-4\log(2)\left(\frac{\left(t-\tau/2\right)^2}{\tau^2}\right)\right) & ;0 \le t \le \tau \\ 0 & ;\tau \le t \le 1/f \end{cases} \tag{4}$$

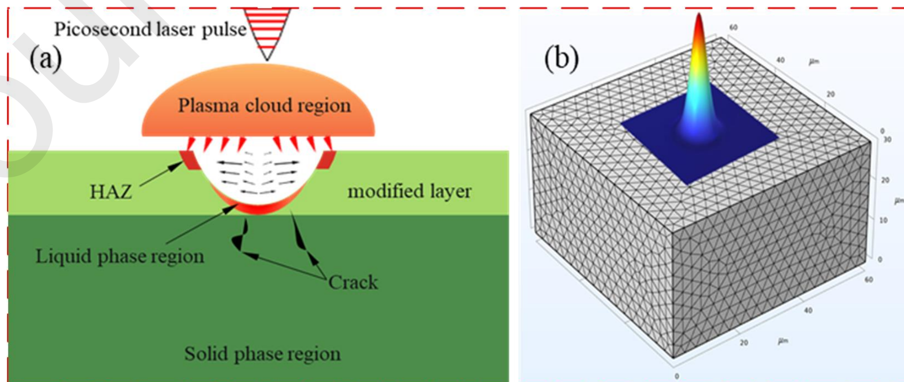

Fig. 5 Schematic diagram of laser modification: (a) laser ablation state; (b) gaussian heat source distribution.

Journal Pre-proofs

4. Result and discussion

4.1 Surface modification of 4H-SiC

4.1.1Effect of PLM on SiC surface roughness

To obtain the laser modification process of the 4H-SiC surface layer, this paper firstly analyses in depth the influence law of laser energy density (above the ablation threshold of 2.67 J/cm^2) on the morphology of SiC material. Fig. 6 displays the surface morphology and corresponding contour curves of SiC following laser processing. The surface roughness (Ra) value of SiC was found to be 674.4 nm when the laser energy density was 4 J/cm^2 (Fig. 6a). With the increase in energy density (Fig. 6b-c), Ra continues to rise to 1985 nm, a trend consistent with the experimental findings of Li et al [28]. It has been demonstrated that when the laser energy density exceeds the SiC ablation threshold, higher energy densities result in the generation of more evaporated particles on the SiC surface. These particles deposit on the SiC surface due to the temperature difference between the recoil pressure and atmospheric pressure, subsequently increasing the number of surface debris and further elevating the Ra [29]. It is noteworthy that at a laser energy density of 16 J/cm^2, the Ra value decreases to 1298.8 nm (Fig. 6d). According to the principle of pulsed laser deposition dynamics [30], the density of particles evaporated by laser irradiation can reach as high as 10^{16} to 10^{27} cm^{-3} when the laser energy density exceeds 10^9 W/m^2. In this article, the laser energy density of 16 J/cm^2 can reach 1.59×10^{16} W/m^2, significantly higher than 10^9 W/m^2. At this moment, the plasma absorbs laser energy via inverse bremsstrahlung radiation, resulting in a significant plasma shielding effect. This leads to the absorption of energy at the centre of the laser spot by the plasma (Fig. 6a), consequently reducing the disparity in energy density between the centre and edges of the spot, and hence reducing Ra. Furthermore, under the same experimental conditions, the shielding effect is stronger at 16 J/cm^2 and inversely proportional to the modification rate. A significant shielding effect occurs at the entrance of the modification slot, where the diffraction effect alters the laser spot position and energy distribution, further reducing the modification rate as depth increases [31-33]. This is why the decrease in surface roughness (Ra) is relative to that at 12 J/cm^2. Therefore, the results of this experiment show that the Ra of SiC increases and then decreases with the increase of laser irradiation energy density.

Journal Pre-proofs

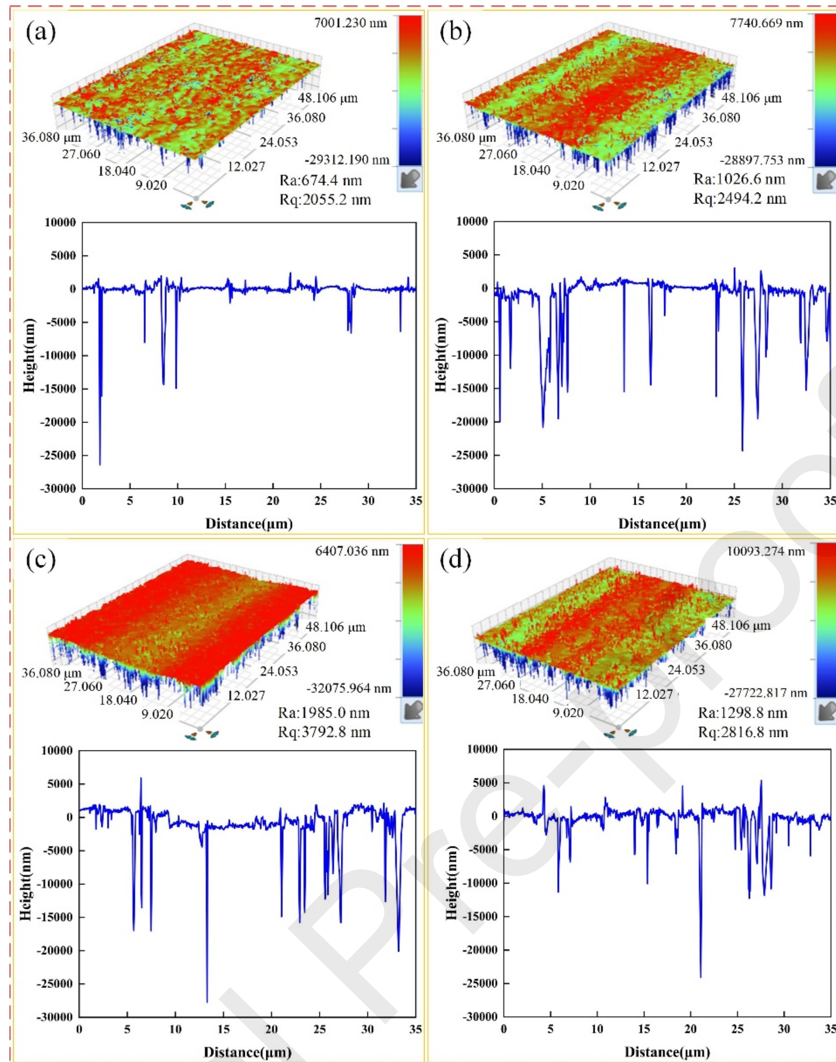

Fig. 6 Surface morphology of laser-modified SiC wafers: (a) 4 J/cm^2; (b) 8 J/cm^2; (c) 12 J/cm^2; (d) 16 J/cm^2.

4.1.2 Effect of PLM on SiC surface morphology

The laser modification mechanism of SiC can be initially explored by observing the surface microstructure changes. Fig. 7 demonstrates the microstructure morphology and elemental content changes of SiC modified by laser. As shown in Fig. 7a, when the laser energy density is 4 J/cm^2, the SiC surface shows a uniform periodic ripple structure with damage cracks (Fig. 7a1). However, as the laser energy density ranges from 8 J/cm2 to 16 J/cm2, the ripple structure on the SiC surface gradually disappears, as shown in Fig. 6b-d. The results show a strong dependence of the periodic ripple structure on the laser energy density [34]. Moreover, Figs. 7b1-d1 reveals the presence of numerous debris and densely clustered particles in the SiC surface deposition layer. This phenomenon can be explained by referring to a typical P-T phase diagram (Fig. 8). The figure illustrates that the equilibrium line of the liquid-vapor system begins at the three-phase point and ends at the critical point (CP). As the transient temperature increases and approaches the CP during laser modification of SiC, the matter undergoes increasingly significant fluctuations. Transient heat accumulation inevitably causes the system to overheat beyond the boiling temperature. At this stage, the system transitions

from equilibrium to the substable region, where the superheated liquid transforms into a mixture of liquid and vapour and evaporates [35, 36]. Additionally, as the heating rate increases, the system approaches the spinodal line. The thermodynamic parameters near the CP become highly unstable, leading to explosive boiling to restore equilibrium of the system [37-39]. Therefore, considering the comprehensive evaluation of the SiC surface microstructure and material removal mechanisms, it can be attributed to the fact that the SiC laser modification mechanism is controlled by a combination of phase explosion and normal superheated melting.

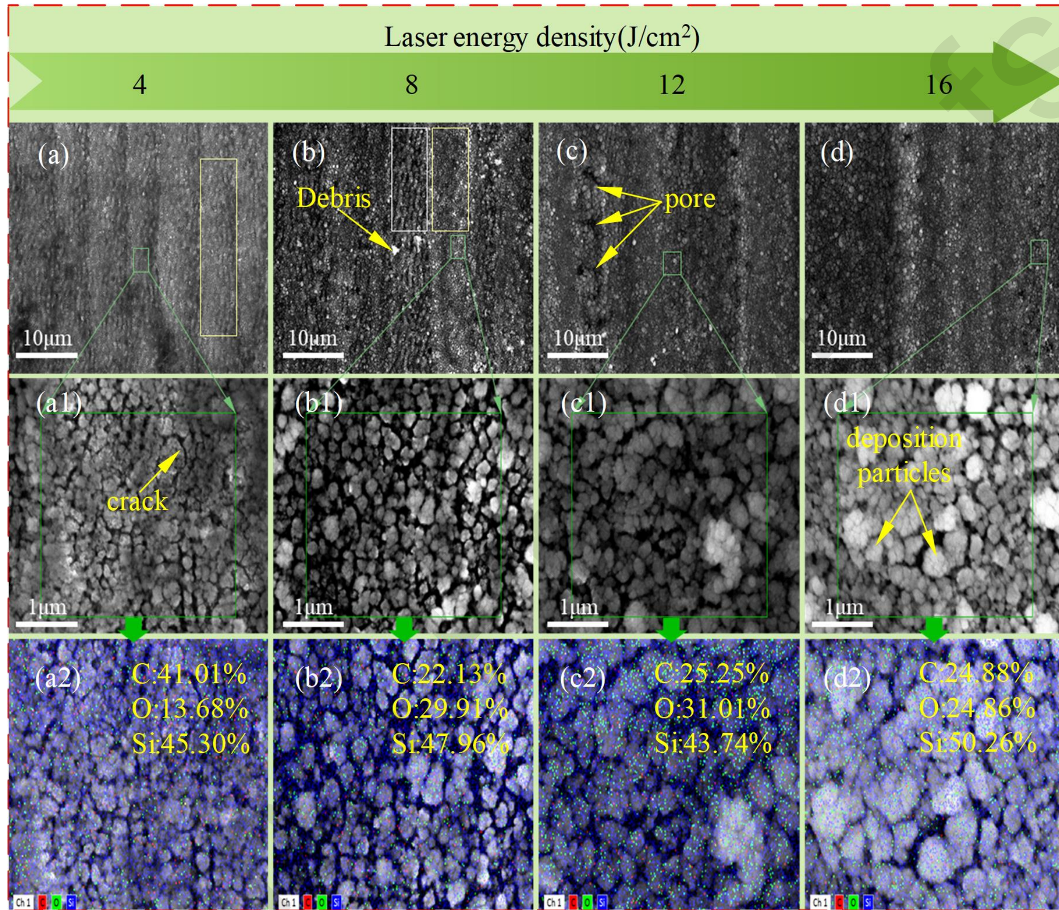

Fig. 7 SEM morphology of laser-modified 4H-SiC: (a-d) SEM morphology; (a2-d2) SEM magnified image; (a2-d2) EDS morphology.

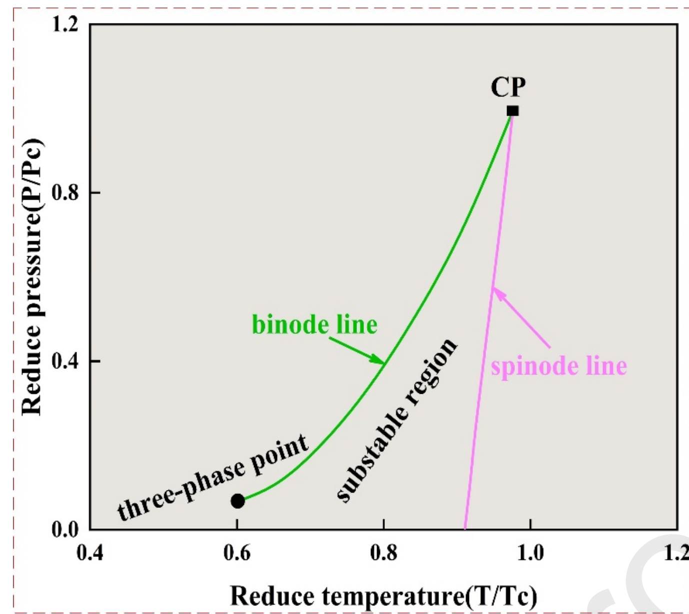

Fig. 8 P–T diagram near the critical point (CP) [37-39]

To provide a deeper insight into the laser-modified behaviour, the chemical composition of the laser-modified SiC surface was investigated. EDS detection was performed on the selected areas in the 6a-d diagram. Figs. 7a2-d2 shows the relative content of surface oxides. The oxide consists mainly of traces of O, Si and C. With the increase in laser energy density, laser modification results in a continuous increase in O content and a significant decrease in C content. However, according to the percentages shown in fig. 7, it seems that the O and C content don't follow a continuous trend (Please refer to Supplementary file 2 for specific reasons). Since the modification is carried out in an atmospheric environment, the reactions of Eq. 5-7 take place when the modification temperature exceeds 3500 °C, exhibiting significant oxidation [40, 41]. The occurrence of oxidative behaviour can also be demonstrated through the surface pores in Fig. 7a-c. Furthermore, as the evaporated particles (containing gaseous silicon oxide) react further with oxygen, a portion is deposited on the surface to form a granular material, as shown in Eq. 8. During this process, the recoil pressure generated by the extremely high laser energy density produces additional evaporated particles. Additionally, due to laser shielding, the modified surface deposits a more uniform particle density (Fig. 7d1), which also contributes to the reduction in surface roughness Ra. Moreover, significant gas escapes due to higher cooling rates, resulting in a decrease in elemental O content [42]. Hence, it can be inferred that SiO_2 is the primary component of the surface oxide.

$$SiC(s)+O_2(g)\rightarrow SiO_2(l)+CO(g) \quad (5)$$

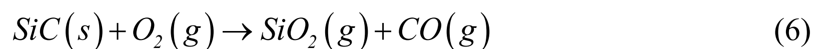

$$SiC(s)+O_2(g)\rightarrow SiO_2(g)+CO(g) \quad (6)$$

$$SiC(s)+O_2(g)\rightarrow SiO(g)+CO(g) \quad (7)$$

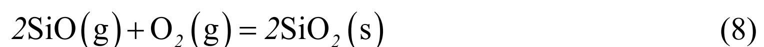

$$2SiO(g)+O_2(g)=2SiO_2(s) \quad (8)$$

4.2 Subsurface characteristic of 4H-SiC

4.2.1 Effect of PLM on SiC Subsurface morphology

The effect of SiC subsurface damage on the mechanical, electronic and optical

properties of the device is irreversible. Therefore, it is imperative to analyse the causes of subsurface damage to SiC resulting from laser modification. Fig. 9 displays the SEM morphology of the subsurface obtained using the angle polishing method after laser modification. As depicted in Fig. 9a, the subsurface exhibits prominent pits and cracks, with the cracks aligned parallel to the direction of the grooves. The non-uniform temperature field and deformation constraints generate a stress gradient in the SiC subsurface, potentially leading to the formation of microcracks that can propagate to rupture when the thermal stress exceeds the fracture strength of SiC [43]. Furthermore, evident air pores were observed at the bottom of the grooves in Fig. 9b, supporting the material modification mechanism outlined in section 4.1.2. The results depicted in Fig. 9c reveal a distinct microporous structure in the subsurface with no apparent cracks. It is noteworthy that the micropores on the subsurface show a disordered distribution as a result of large overlap rates irradiated multiple times on the same unit area. The molten material experiences multiple reflections and scattering as a consequence of the downward shift of the focal plane induced by the thermal effects of neighbouring pulses. This process ultimately leads to the formation of a disordered microporous morphology. In addition, narrow cracks can be found in Fig. 9d. As described in the literature [44, 45], the crack damage observed in the subsurface is closely associated with the thermal stresses induced during laser irradiation.

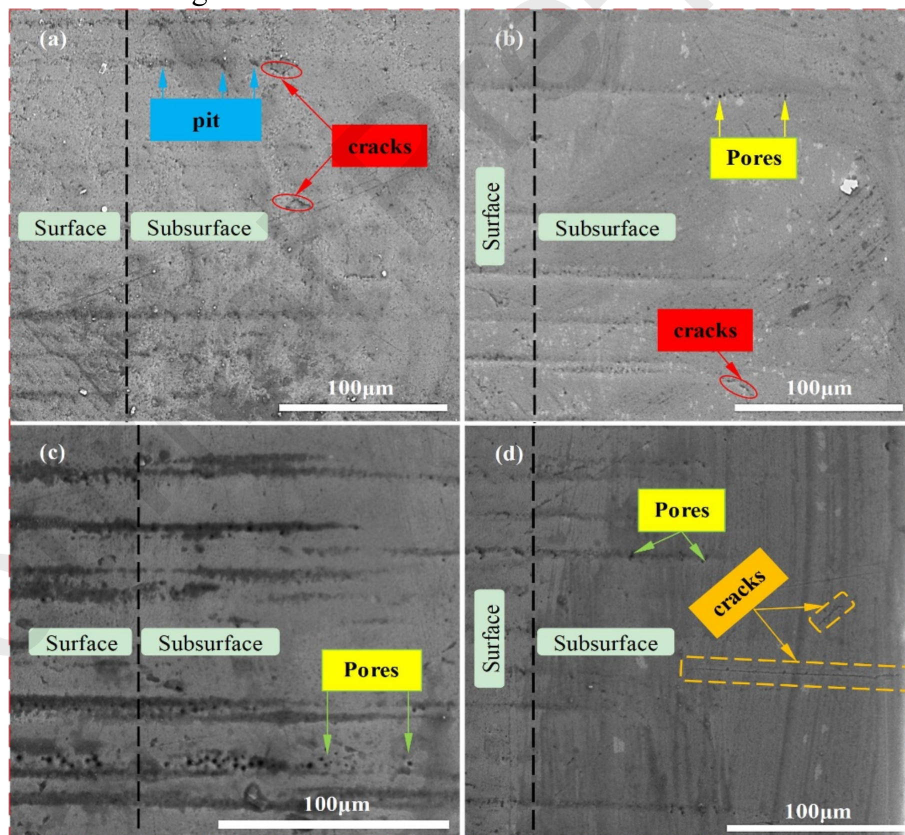

Fig. 9 Subsurface characteristics obtained through angle polishing method: (a) 4 J/cm^2; (b) 8 J/cm^2; (c) 12 J/cm^2; (d) 16 J/cm^2.

Analyzing the evolution of the temperature field is an effective approach to further understanding the emergence of cracks on laser-modified subsurface. Fig. 10 shows the distribution state of the temperature field with increasing laser energy density. With

increasing laser energy density, the modification depth gradually increases, consistent with the proportional relationship between laser energy and modification depth. The simulation results indicate that the temperature at the centre of the spot can reach up to 3200 K, exceeding the evaporation temperature of SiC. This aligns with the high-temperature evaporation conditions necessary for the material modification mechanism discussed in Section 4.1.2. On the other hand, the instantaneous high temperature of the laser modification and the rapid cooling after the laser disappears, lead to a higher thermal stress gradient at the subsurface. Cracks occur when the stress exceeds the fracture strength of SiC, which is the underlying cause of the cracks depicted in Fig. 9a. Therefore, the irregular cracks in the exposed position of the subsurface were caused by the volume change of the material due to multiple melting-cooling-melting cycles resulting from the overlapping behaviour of the laser.

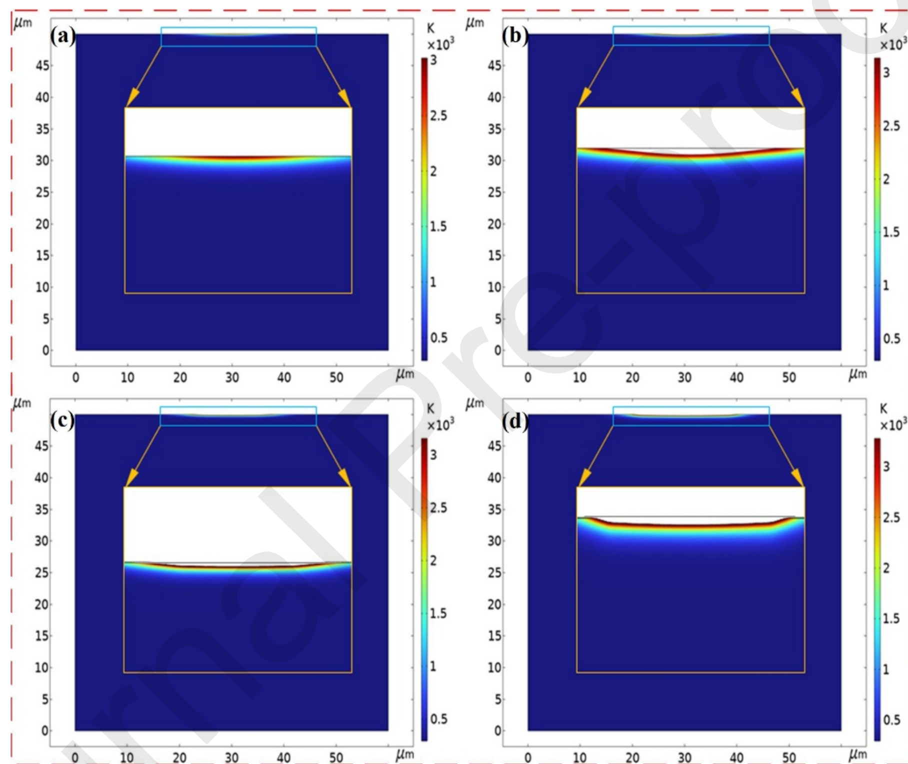

Fig. 10 The simulated temperature field under the single laser pulse energy: (a) 4 J/cm^2; (b) 8 J/cm^2; (c) 12 J/cm^2; (d) 16 J/cm^2.

4.2.2 Subsurface XPS analysis

The chemical composition of the laser-modified subsurface plays a crucial role in comprehending the subsurface damage mechanism. The detection results of SiC subsurface XPS before and after modification (with increasing laser energy density) are shown in Fig. 11. Fig. 11a displays the full spectrum of XPS detection, indicating a significant change in the peak intensity of the relative atomic percentage of the subsurface with increasing energy density. The intensity of both C1s and Si2p decreased after laser modification, with the decrease in Si2p peak intensity being larger than that of C1s, while the peak intensity of O1s increased. This suggests significant changes in the content and concentration of subsurface elements after laser modification. In contrast, at a laser power of 20 W, the opposite result to the 5-15 W phenomenon

occurs (O1s and Si2p intensities decrease, and C1s intensity increases). This is because the laser's shielding effect reduces active oxidation at the laser centre, resulting in less gas production (Eq. 7). Additionally, gases trapped during the material's melt flow do not escape during rapid cooling (Eq. 8), leading to their deposition on the 4H-SiC surface. Thus, XPS results differ from those observed at 5-15 W.

Fig. 11b and c show the energy spectra of C1s, O1s and Si2p at laser energy densities of 4 J/cm^2 and 16 J/cm^2, respectively. The C1s spectrum before modification shows two peaks at positions 284.8 eV and 285.8 eV for Si-C and C-C, respectively. In the O1s spectrum, the major and secondary peaks appear at 533.2 eV and 534.3 eV, corresponding to Si-O and C-O bonds, respectively. In the Si2p spectrum, 101.2 eV and 102.1 eV correspond to peaks at the Si=C and Si-O bond positions, respectively. The corresponding peak intensities of the O1s and Si2p spectra indicate that the exposure of pristine 4H-SiC to air resulted in the oxidation of a small portion of the surface [46]. The C1s and Si2p spectra of the angle-polished surfaces after modification decrease dramatically, indicating a large-scale breakdown of the 4H-SiC crystal structure and a decrease in Si and C concentrations. In addition, the enhanced peak intensity at position 102.1 eV in the Si2p spectrum and the sharp increase in the O1s spectrum indicate the generation of SiO_2 as a new substance. The above changes indicate that the action of the polishing solution during the angular polishing process leads to the formation of a large amount of SiO_2 in reaction with the SiC substrate after the removal of the laser-modified layer.

Journal Pre-proofs

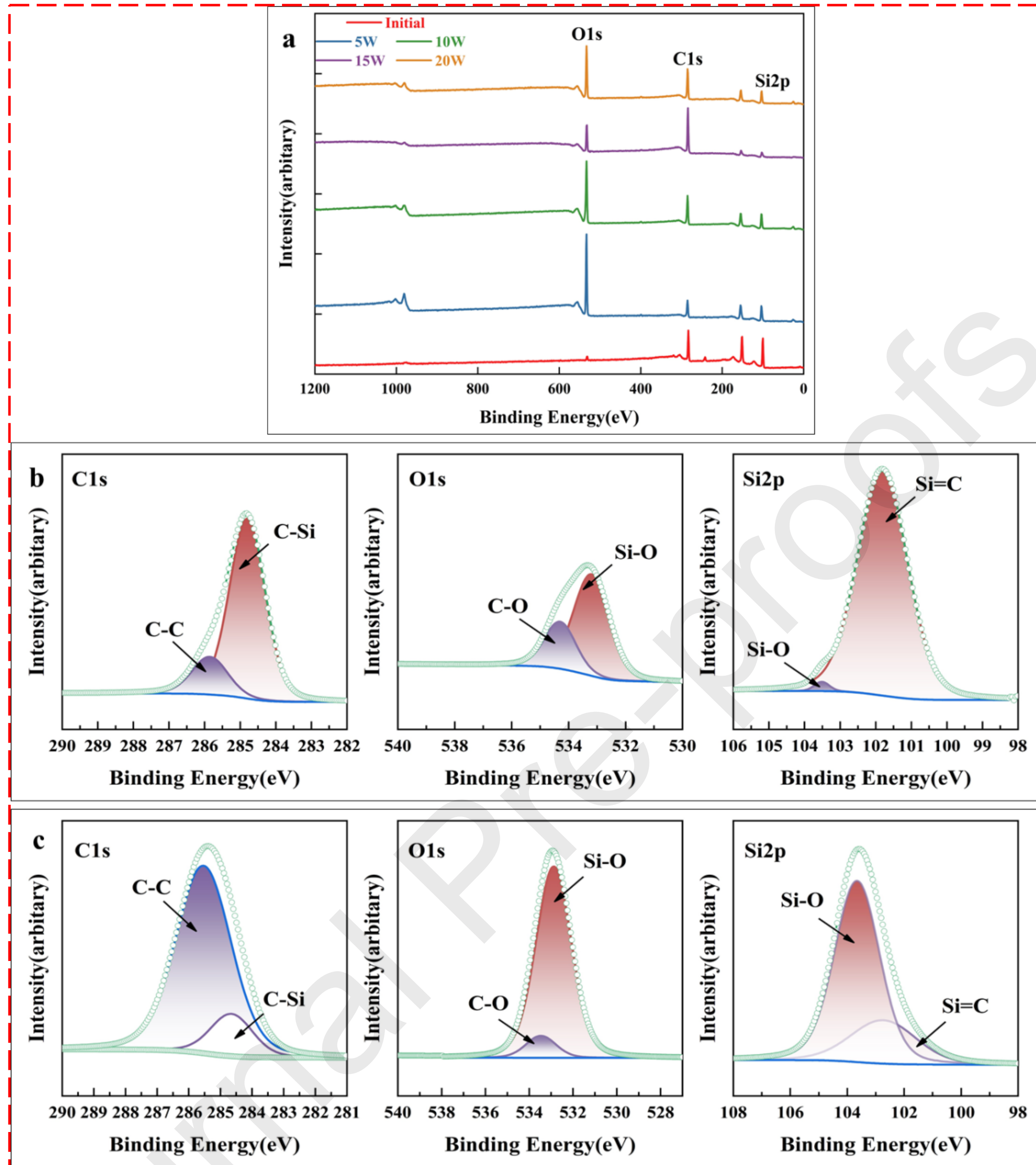

Fig. 11 XPS spectra of 4H-SiC after angle polishing: (a) Full spectrum; (b) fine spectrum of 4 J/cm^2; (c) fine spectrum of 16 J/cm^2.

4.3 Mechanical properties of 4H-SiC

Fig. 12a depicts the load-displacement curves measured on Si surfaces with laser energy densities of 4, 8, 12, and 16 J/cm^2, along with that on the pristine SiC surface. The nanoindentation hardness was measured using a nanoindentation tester (G200) with a Berkovich-type indentation tip and a maximum load of 500 mN. The load stay time was 10s and the loading/unloading rate was 10mN/s. From Fig. 12a, it is evident that the load-displacement curves exhibit a clear inflexion phenomenon (indicated by the arrows in the figure, referred to as pop-ins and pop-outs), suggesting that SiC experienced plastic deformation during the nanoindentation process following laser modification. The load-displacement curves after laser irradiation were shifted to the right, indicating that the laser modification reduced the nanoindentation hardness of the

sample surface and improved the machinability of the SiC. In addition, the laser-modified surface periodic structure and pore characteristics result in relatively gentle slopes at low load states. Fig. 12b shows the relationship between the average nanoindentation hardness (averaged over three repetitions) and energy density for SiC. The average nanoindentation hardness of the pristine SiC surface was 36.9 GPa, and 20.7, 7.7, 3.6 and 2.4 GPa after laser modification, respectively. The results show that the surface hardness decreases with the increase of laser energy density, which is helpful for the subsequent ultra-precision machining efficiency and surface quality of SiC.

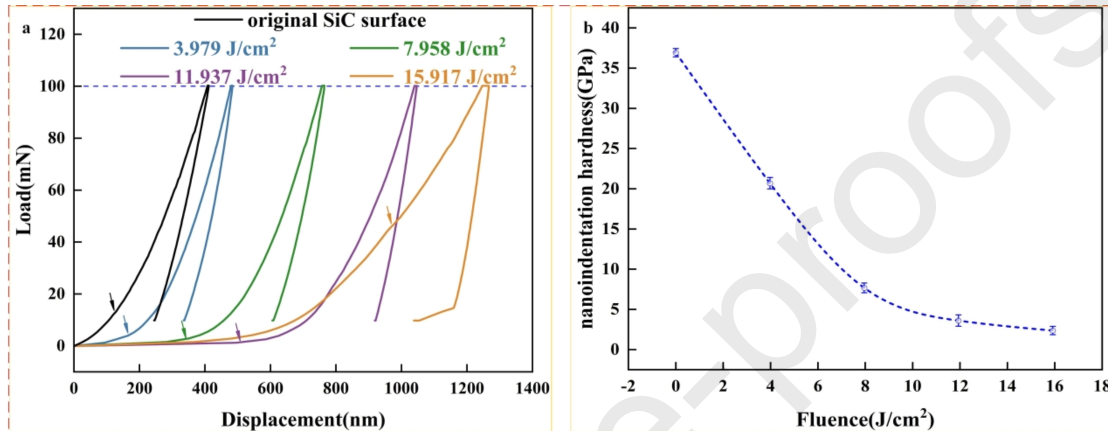

Fig. 12 Indentation load-displacement curves of the original and laser-irradiated a. b, Variation of the averaged nanoindentation hardness of the laser-irradiated.

5. Conclusion

The inherent properties of 4H-SiC severely restrict its application as a high-performance device. Therefore, the investigation into the laser-induced modification of 4H-SiC serves as a crucial reference for enhancing the efficiency and minimizing subsurface damage in future chemical-mechanical polishing processes. This paper systematically investigates the laser-induced surface layer modification and subsurface damage mechanism of 4H-SiC, contributing positively to the advancement of the theoretical framework for laser modification of 4H-SiC. The main conclusions are summarized as follows:

(1) The surface morphology of SiC after laser modification under the experimental conditions indicates that the shielding effect resulting from laser heat accumulation leads to a decrease in Ra. Additionally, from the analysis of thermodynamic theory and laser-modified results, it is evident that recast layers and particles form on the surface of SiC due to the mixture of liquid and vapour produced when the laser temperature reaches the thermodynamic critical point. Hence, the mechanism of laser modification is believed to involve phase explosion and normal superheated melting induced by heat accumulation.

(2) The damage mechanisms in the subsurface of 4H-SiC during laser-induced processes include cracks and structural changes. The cracking behaviour is primarily concentrated in the recast, with tensile stresses generated by laser action and volumetric changes in the molten material resulting from the overlap behaviour between adjacent spots (alternating hot-cold cycles) are the main causes of the cracking.

(3) According to the XPS test results before and after laser modification, the sub-

Journal Pre-proofs

surface of laser-modified SiC exhibits evident oxidation, leading to significant damage and transformation of the monocrystalline structure into SiO_2. Moreover, laser modification effectively reduces the hardness of SiC, enhancing its machinability. These findings offer theoretical support for subsequent ultra-precision machining of SiC to achieve higher material removal rates and superior surface quality.

Haixu Liu: Writing – original draft, Visualization, Software, Methodology, Investigation, Data curation. Zhipeng Li: Writing – review & editing, Validation, Supervision, Methodology, Investigation. Ping Zhang: Investigation, Conceptualization. Dunwen Zuo: Supervision, Resources, Funding acquisition. Wenkun Xie: Guide, Review & editing.

Data availability

Data will be made available on request.

Declaration of competing interest

The authors declare that they have no known competing financial interests or personal relationships that could have appeared to influence the work reported in this paper.

Acknowledgements

This work was supported by the Joint Funds of the National Natural Science Foundation of China (Grant No. U20A20293), the National Natural Science Foundation of China (No. 52205478), Basic Research Programs of Natural Science Foundation of Jiangsu Province (No. BK20220891). Supported by National Key Laboratory of Science and Technology on Helicopter Transmission (No. HTL-A-22G04).

References

[1] A.S. Kashyap, C.P. Chen, R. Ghandi, A. Patil, E. Andarawis, L. Yin, D. Shaddock, P. Sandvik, K. Fang, Z.Z. Shen, W. Johnson, Silicon Carbide Integrated Circuits for Extreme Environments, Wide Bandgap Power Devices and Applications (Wipda), (2013) 60-63. http://doi.org/10.1109/WiPDA.2013.6695562

[2] C.R. L.d. Jiang, A review of silicon carbide development in MEMS applications, International Journal of Computational Materials Science and Surface Engineering, 2(3-4) (2009) 227-242. http://doi.org/10.1504/IJCMSSE.2009.027484

[3] Y.G. Huang, F. Tang, Z. Guo, X.H. Wang, Accelerated ICP etching of 6H-SiC by femtosecond laser modification, Appl Surf Sci, 488 (2019) 853-864. http://doi.org/10.1016/j.apsusc.2019.05.262

[4] M. Wu, H. Huang, Q.F. Luo, Y.Q. Wu, A novel approach to obtain near damage-free surface/subsurface in machining of single crystal 4H-SiC substrate using pure metal mediated friction, Appl Surf Sci, 588 (2022). http://doi.org/10.1016/j.apsusc.2022.152963

[5] H. Deng, K. Endo, K. Yamamura, Competition between surface modification and abrasive polishing: a method of controlling the surface atomic structure of 4H-SiC (0001), Sci Rep, 5 (2015) 8947. http://doi.org/10.1038/srep08947

[6] J. Yan, X. Gai, H. Harada, Subsurface damage of single crystalline silicon carbide in nanoindentation tests, J Nanosci Nanotechnol, 10 (2010) 7808-7811. http://doi.org/10.1166/jnn.2010.2895

[7] G. Pan, Y. Zhou, G. Luo, X. Shi, C. Zou, H. Gong, Chemical mechanical polishing

Journal Pre-proofs

(CMP) of on-axis Si-face 6H-SiC wafer for obtaining atomically flat defect-free surface, Journal of Materials Science: Materials in Electronics, 24 (2013) 5040-5047. http://doi.org/10.1007/s10854-013-1519-1
[8] J. Lu, Y. Huang, Y. Fu, Q. Yan, S. Zeng, Synergistic Effect of Photocatalysis and Fenton on Improving the Removal Rate of 4H-SiC during CMP, ECS Journal of Solid State Science and Technology, 10(4) (2021) 044001. http://doi.org/10.1149/2162-8777/abf16d
[9] Y. Ein-Eli, D. Starosvetsky, Review on copper chemical-mechanical polishing (CMP) and post-CMP cleaning in ultra large system integrated (ULSI) - An electrochemical perspective, Electrochim Acta, 52 (2007) 1825-1838. http://doi.org/10.1016/j.electacta.2006.07.039
[10] H. Deng, N. Liu, K. Endo, K. Yamamura, Atomic-scale finishing of carbon face of single crystal SiC by combination of thermal oxidation pretreatment and slurry polishing, Appl Surf Sci, 434 (2018) 40-48. http://doi.org/10.1016/j.apsusc.2017.10.159
[11] C.-H. Hsieh, C.-Y. Chang, Y.-K. Hsiao, C.-C.A. Chen, C.-C. Tu, H.-C. Kuo, Recent Advances In Silicon Carbide Chemical Mechanical Polishing Technologies, Micromachines, 13 (2022). http://doi.org/10.3390/mi13101752
[12] X.C. Yin, S.J. Li, G.L. Ma, Z. Jia, X. Liu, Investigation of oxidation mechanism of SiC single crystal for plasma electrochemical oxidation, Rsc Adv, 11 (2021) 27338-27345. http://doi.org/10.1039/d1ra04604g
[13] J.Y. Long, Q.F. Peng, G.P. Chen, Y.L. Zhang, X.Z. Xie, G.S. Pan, X.F. Wang, Centimeter-scale low-damage micromachining on single-crystal 4H-SiC substrates using a femtosecond laser with square-shaped Flat-Top focus spots, Ceram Int, 47 (2021) 23134-23143. http://doi.org/10.1016/j.ceramint.2021.05.027
[14] R.R. Gattass, E. Mazur, Femtosecond laser micromachining in transparent materials, Nat Photonics, 2 (2008) 219-225. http://doi.org/10.1038/nphoton.2008.47
[15] Y.H. Huang, Y.Q. Zhou, J.M. Li, F.L. Zhu, Femtosecond laser surface modification of 4H-SiC improves machinability, Appl Surf Sci, 615 (2023). http://doi.org/10.1016/j.apsusc.2023.156436
[16] D.C. Qin, J.W. Wu, J.W. Li, Y.C. Ma, M.H. Ye, D. Tian, C. Wang, F. Ji, Effect of femtosecond laser modification on magnetorheological finishing of magnesium aluminate spinel, Int J Adv Manuf Tech, 125 (2023) 2593-2600. http://doi.org/10.1007/s00170-023-10924-1
[17] W. Amsellem, H.Y. Sarvestani, V. Pankov, Y. Martinez-Rubi, J. Gholipour, B. Ashrafi, Deep precision machining of SiC ceramics by picosecond laser ablation, Ceram Int, 49 (2023) 9592-9606. http://doi.org/10.1016/j.ceramint.2022.11.129
[18] E.G. Zahrani, M. Paknejad, A. Zahedi, B. Azarhoushang, Investigation of laser-assisted cylindrical grinding of silicon nitride ceramics with controlled damage zone, Opt Laser Technol, 174 (2024). http://doi.org/10.1016/j.optlastec.2024.110616
[19] P. Molian, B. Pecholt, S. Gupta, Picosecond pulsed laser ablation and micromachining of 4H-SiC wafers, Appl Surf Sci, 255 (2009) 4515-4520. http://doi.org/10.1016/j.apsusc.2008.11.071
[20] C. Wu, X.D. Fang, Q. Kang, H. Sun, L.B. Zhao, B. Tian, Z.Y. Fang, M.L. Pan, R.

Journal Pre-proofs

Maeda, Z.D. Jiang, Crystal cleavage, periodic nanostructure and surface modification of SiC ablated by femtosecond laser in different media, Surf Coat Tech, 424 (2021). http://doi.org/10.1016/j.surfcoat.2021.127652
[21] H.J. An, J.S. Wang, H.Y. Cui, F.Z. Fang, Periodic surface structure of 4H-SiC by 46.9 nm laser, Opt Express, 31 (2023) 15438-15448. http://doi.org/10.1364/Oe.487761
[22] X.Z. Xie, Q.F. Peng, G.P. Chen, J.G. Li, J.Y. Long, G.S. Pan, Femtosecond laser modification of silicon carbide substrates and its influence on CMP process, Ceram Int, 47 (2021) 13322-13330. http://doi.org/10.1016/j.ceramint.2021.01.188
[23] B.B. Meng, J. Zheng, D.D. Yuan, S.L. Xu, Machinability improvement of silicon carbide via femtosecond laser surface modification method, Appl Phys a-Mater, 125 (2019). http://doi.org/10.1007/s00339-018-2377-8
[24] R.S. Wei, S. Song, K. Yang, Y.X. Cui, Y. Peng, X.F. Chen, X.B. Hu, X.G. Xu, Thermal conductivity of 4H-SiC single crystals, J Appl Phys, 113 (2013). http://doi.org/10.1063/1.4790134
[25] S.G. Muller, R. Eckstein, J. Fricke, D. Hofmann, R. Hofmann, R. Horn, H. Mehling, O. Nilsson, Experimental and theoretical analysis of the high temperature thermal conductivity of monocrystalline SiC, Mater Sci Forum, 264-2 (1998) 623-626. http://doi.org/10.4028/www.scientific.net/MSF.264-268.623
[26] V. Tangwarodomnukun, J. Wang, C.Z. Huang, H.T. Zhu, Heating and material removal process in hybrid laser-waterjet ablation of silicon substrates, International Journal of Machine Tools & Manufacture, 79 (2014) 1-16. http://doi.org/10.1016/j.ijmachtools.2013.12.003
[27] H. Zhu, Z.Y. Zhang, J.Z. Zhou, K. Xu, D.Y. Zhao, V. Tangwarodomnukun, A computational study of heat transfer and material removal in picosecond laser micro-grooving of copper, Optics and Laser Technology, 137 (2021). http://doi.org/10.1016/j.optlastec.2020.106792
[28] J. Li, L.F. Ji, Y. Hu, Y. Bao, Precise micromachining of yttria-tetragonal zirconia polycrystal ceramic using 532 nm nanosecond laser, Ceramics International, 42 (2016) 4377-4385. http://doi.org/10.1016/j.ceramint.2015.11.118
[29] A. De Zanet, V. Casalegno, M. Salvo, Laser surface texturing of ceramics and ceramic composite materials - A review, Ceramics International, 47 (2021) 7307-7320. http://doi.org/10.1016/j.ceramint.2020.11.146
[30] D. Zhang, Dynamic principles of pulsed laser deposition, in: Beijing Science and Technology Press, 2011.
[31] P.M. Jean-Philippe Desbiens, ArF excimer laser micromachining of Pyrex, SiC and PZT for rapid prototyping of MEMS components, Sensors and Actuators A: Physical, 136 (2007). http://doi.org/10.1016/j.sna.2007.01.002
[32] A.A. Tseng, Y.T. Chen, K.J. Ma, Fabrication of high-aspect-ratio microstructures using excimer laser, Opt Laser Eng, 41 (2004) 827-847. http://doi.org/10.1016/S0143-8166(03)00062-9
[33] S. Gupta, B. Pecholt, P. Molian, Excimer laser ablation of single crystal 4H-SiC and 6H-SiC wafers, J Mater Sci, 46 (2011) 196-206. http://doi.org/10.1007/s10853-010-4920-7
[34] J.Y. Long, Z.Y. He, D.Y. Ou, Y.J. Huang, P.C. Wang, Q.L. Ren, X.Z. Xie,

Journal Pre-proofs

Formation of dense nanostructures on femtosecond laser-processed silicon carbide surfaces, Surfaces and Interfaces, 28 (2022). http://doi.org/10.1016/j.surfin.2021.101624
[35] D. von der Linde, K. Sokolowski-Tinten, The physical mechanisms of short-pulse laser ablation, Applied Surface Science, 154 (2000) 1-10. http://doi.org/10.1016/S0169-4332(99)00440-7
[36] K.H. Song, X.F. Xu, Explosive phase transformation in excimer laser ablation, Appl Surf Sci, 127 (1998) 111-116. http://doi.org/10.1016/S0169-4332(97)00619-3
[37] S. Eliezer, N. Eliaz, E. Grossman, D. Fisher, I. Gouzman, Z. Henis, S. Pecker, Y. Horovitz, M. Fraenkel, S. Maman, Y. Lereah, Synthesis of nanoparticles with femtosecond laser pulses, Physical Review B, 69 (2004). http://doi.org/10.1103/PhysRevB.69.144119
[38] N.M. Bulgakova, A.V. Bulgakov, Pulsed laser ablation of solids: transition from normal vaporization to phase explosion, Applied Physics a-Materials Science & Processing, 73 (2001) 199-208. http://doi.org/10.1007/s003390000686
[39] B. Pecholt, M. Vendan, Y. Dong, P. Molian, Ultrafast laser micromachining of 3C-SiC thin films for MEMS device fabrication, International Journal of Advanced Manufacturing Technology, 39 (2008) 239-250. http://doi.org/10.1007/s00170-007-1223-5
[40] S.N. Pan, Q.Y. Li, Z.K. Xian, N.G. Su, F.Z. Zeng, The Effects of Laser Parameters and the Ablation Mechanism in Laser Ablation of C/SiC Composite, Materials, 12 (2019). http://doi.org/10.3390/ma12193076
[41] L. Liu, H.J. Li, W. Feng, X.H. Shi, K.Z. Li, L.J. Guo, Ablation in different heat fluxes of C/C composites modified by ZrB-ZrC and ZrB-ZrC-SiC particles, Corrosion Science, 74 (2013) 159-167. http://doi.org/10.1016/j.corsci.2013.04.038
[42] S.C. Feng, R. Zhang, C.Z. Huang, J. Wang, Z.X. Jia, J. Wang, An investigation of recast behavior in laser ablation of 4H-silicon carbide wafer, Materials Science in Semiconductor Processing, 105 (2020). http://doi.org/10.1016/j.mssp.2019.104701
[43] Z. Zhang, Q.L. Zhang, Q.W. Wang, H.H. Su, Y.C. Fu, J.H. Xu, Investigation on the material removal behavior of single crystal diamond by infrared nanosecond pulsed laser ablation, Optics and Laser Technology, 126 (2020). http://doi.org/10.1016/j.optlastec.2020.106086
[44] D.J. Wu, F. Lu, D.K. Zhao, G.Y. Ma, C.J. Li, J. Ding, F.Y. Niu, Effect of doping SiC particles on cracks and pores of AlO-ZrO eutectic ceramics fabricated by directed laser deposition, Journal of Materials Science, 54 (2019) 9321-9330. http://doi.org/10.1007/s10853-019-03555-z
[45] S.K. Ghosh, P. Saha, Crack and wear behavior of SiC particulate reinforced aluminium based metal matrix composite fabricated by direct metal laser sintering process, Materials & Design, 32 (2011) 139-145. http://doi.org/10.1016/j.matdes.2010.06.020
[46] M. Sreemany, T.B. Ghosh, B.C. Pai, M. Chakraborty, XPS studies on the oxidation behavior of SiC particles, Materials Research Bulletin, 33 (1998) 189-198. http://doi.org/10.1016/S0025-5408(97)00222-5

Journal Pre-proofs

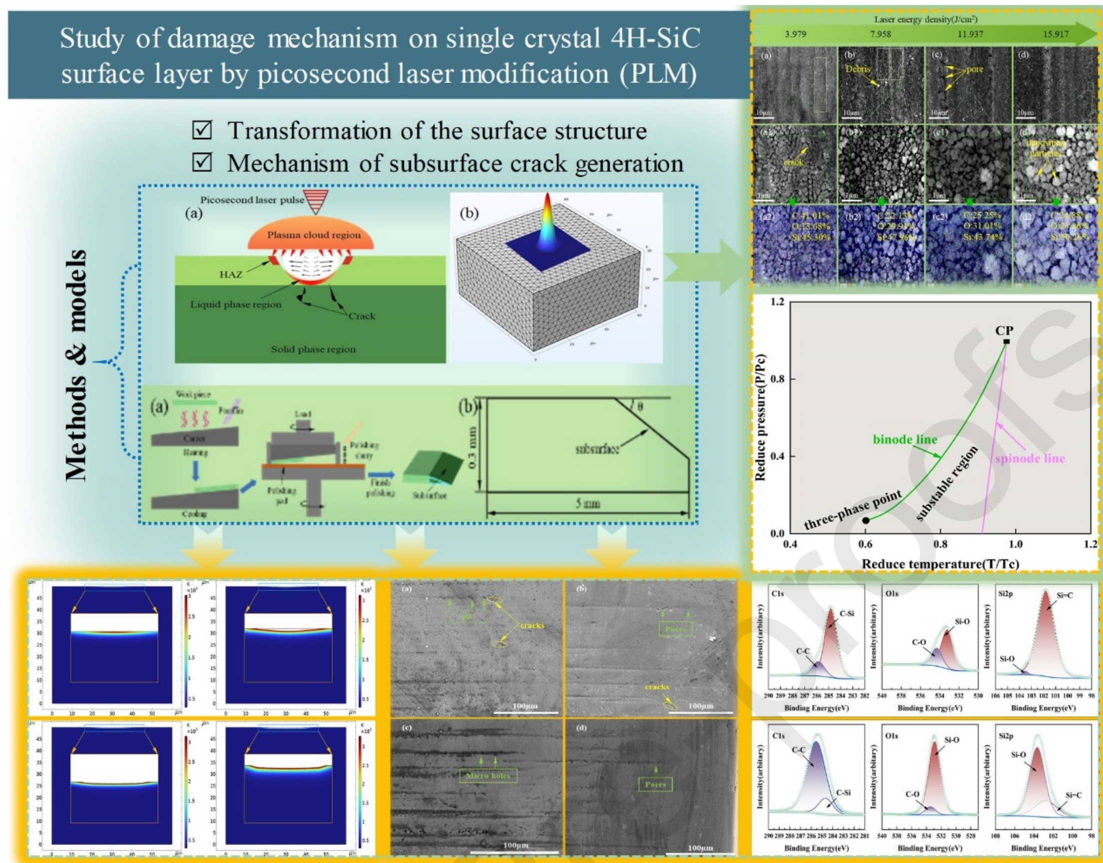

Highlights

- Combination of picosecond laser direct writing and characterization to study the properties of picosecond laser-modified SiC surface layers.
- The evolution of the energy density in relation to the modified layer structure is revealed.
- The reason for the sub-surface damage mechanism of picosecond laser modification is illustrated.
- Laser modification can effectively reduce the hardness of silicon carbide and improve its machinability.

Declaration of interest statement

The authors declare that they have no known competing financial interests or personal relationships that could have appeared to influence the work reported in this paper.

Journal Pre-proofs